

Electron transport at metal-semiconductor interfaces: General theory

R. T. Tung

AT&T Bell Laboratories, Murray Hill, New Jersey 07974

(Received 3 September 1991; revised manuscript received 29 January 1992)

A dipole-layer approach is presented, which leads to analytic solutions to the potential and the electronic transport at metal-semiconductor interfaces with arbitrary Schottky-barrier-height profiles. The presence of inhomogeneities in the Schottky-barrier height is shown to lead to a coherent explanation of many anomalies in the experimental results. These results suggest that the formation mechanism of the Schottky barrier is locally nonuniform at common, polycrystalline, metal-semiconductor interfaces.

I. INTRODUCTION

The formation mechanism of the Schottky barrier (SB) at metal-semiconductor (MS) interfaces is still an unsettled issue despite decades of intensive investigations.^{1,2} Presently, the most popular proposal of SB formation seems to be Fermi-level (FL) pinning by electronic states at the MS interface, such as metal-induced gap states (MIGS's) (Refs. 3 and 4) and defect-related states.⁵⁻⁷ According to the FL pinning proposals, the Schottky-barrier height (SBH) of a MS system should be uniform. However, recent experimental⁸⁻¹¹ and theoretical¹²⁻¹⁴ results from high-quality, epitaxial MS interfaces suggest that the SBH depends on the structure of the MS interface. Such a dependence implies that the SBH of nonepitaxial MS interfaces may be inhomogeneous. Thus, the question whether the SBH varies at MS interfaces has a direct bearing on identifying the formation mechanism of the SB. Recently, it was pointed out that experimental data obtained from the vast majority of MS interfaces are consistent with the presence of SBH inhomogeneity.¹⁵ Hence, existing transport theories, such as the thermionic emission theory and the diffusion theory, are inadequate for a general description of the experimental results, because they are based on the assumption of a homogeneous SBH. In this paper, I present a general theory of electron transport at nondegenerate MS interfaces with arbitrary SBH distributions. Analytic solutions of the potential and the electron transport are discussed in detail and shown explicitly to give an excellent account of a host of experimental observations. A brief summary of the present work has already been published.¹⁵ Additional proof for the present theory, based on numerical solutions to Poisson's equation, is presented elsewhere.¹⁶

Homogeneity of the SBH has thus far been implicitly assumed in the analyses of electrical data obtained from SBH measurements. For example, the current-voltage (I - V) relationship of a SB junction has been described by the thermionic emission theory as¹

$$I(V_a) = I_s \left[\exp \left(\frac{qV_a}{nk_B T} \right) - 1 \right] \\ = I_s \left[\exp \left(\frac{\beta V_a}{n} \right) - 1 \right], \quad (1)$$

where q is the electronic charge, k_B is the Boltzmann constant, T is the absolute temperature, V_a is the applied bias, $\beta \equiv q/(k_B T)$, and I_s is the saturation current, given by

$$I_s = A^* A T^2 \exp(-\beta \Phi_B), \quad (2)$$

where A^* is the Richardson constant and A is the area of the diode. When the SB is homogeneous, Φ_B is the SBH of the junction. The ideality factor, n in Eq. (1), is a fit to the slope of an experimental (semilogarithmic) I - V curve. It is clear that if formulas like Eqs. (1) and (2) are used to analyze any I - V data that have a semilogarithmic relationship, a single parameter Φ_B is obtained which is then regarded as the SBH. However, the validity of Eq. (2) depends on the homogeneity of the SBH. One notes that the vast majority of experiments where Eq. (2) is applied contain no verification on the homogeneity of the SBH.

Traditionally, electron transport at inhomogeneous MS junctions has been treated by a parallel conduction model, namely, the current is assumed to be a sum of the currents flowing in all the individual patches (I_i), each with its own area (A_i) and SBH (Φ_i):

$$I(V_a) = \sum_i I_i = A^* T^2 [\exp(\beta V_a) - 1] \sum_i \exp(-\beta \Phi_i) A_i. \quad (3)$$

Such a concept was so intuitively obvious that this model had been applied many times¹⁷ before it was formally discussed by Ohdomari and Tu.¹⁸ However, the parallel conduction model¹⁸ is in significant error when the SBH varies spatially on a scale less than, or comparable to, the depletion region width. The error arises because Eq. (3) fails to take into account the interaction between neighboring patches with different SBH's.^{19,20} For example, the conduction path in front of a small patch with a low SBH is pinched-off if surrounded by high-SBH patches. "Pinch-off" is a terminology often used to describe the operation of a field effect transistor. In the present context, an area is said to be pinched-off if majority carriers originating from outside the space charge region need to go over a potential barrier, higher than the band-edge position at the MS interface, in order to reach the MS interface. Potential pinch-off at inhomogeneous SB's has thus

far only been demonstrated numerically.^{19,21} It is impractical to solve the boundary-value problems for a large number of parameters, which is necessary for a quantitative explanation of routine experimental data. This paper presents a simple approach which allows an accurate analytic description of the potential and the current flow for an arbitrary SBH distribution.

II. POTENTIAL DISTRIBUTION AT MS INTERFACES

A. The dipole-layer approach

When the SBH varies locally at a MS interface the potential also varies from region to region. A nondegenerate semiconductor, occupying the space $z \geq 0$, is assumed to be in contact with a metal at $z \leq 0$. Without the loss of generality, we may assume the semiconductor to be uniformly n -type doped. All results discussed in the present work also apply to p -type semiconductors, with minor changes in the appropriate subscripts. The solution to such a boundary-value problem is usually obtained by solving Poisson's equation, with SBH contours supplied as the boundary condition,

$$V(x, y, 0) = \Phi_B(x, y) = \Phi_B^0 + \delta(x, y), \quad (4)$$

where V is the potential of the conduction-band minimum (CBM) of the semiconductor, referenced to the FL of the metal, and δ is the difference between the local SBH and a "mean" SBH, Φ_B^0 . In the present approach, we treat the variation of the potential due to the presence of the SBH inhomogeneity as a perturbation. It is obvious that the potential due to a dipole layer with a varying dipole moment per area, $2\epsilon_s \delta(x, y)$, should be used as the perturbative term, since it satisfies the Laplace equation and reproduces the desired boundary condition at the MS interface. In other words, the potential in the depletion region of the semiconductor ($0 < z < W$) is approximately described by

$$V(x, y, z) = V_{bb} \left[1 - \frac{z}{W} \right]^2 + V_n + V_a + \int \frac{\delta(x_1, y_1)}{2\pi} \frac{z}{[z^2 + (x_1 - x)^2 + (y_1 - y)^2]^{3/2}} \times dx_1 dy_1, \quad (5)$$

where V_{bb} is the band bending corresponding to a MS junction with a uniform SBH of Φ_B^0 ($V_{bb} = \Phi_B^0 - V_n - V_a$), W , defined as $(2\epsilon_s V_{bb} / qN_D)^{1/2}$, is the depletion width, and V_n is the difference between the FL and the CBM for neutral semiconductor [$V_n = \beta^{-1} \ln(N_C / N_D)$]. The first three terms on the right-hand side of Eq. (5) represent the potential, within the depletion approximation, due to a uniform SBH of Φ_B^0 .¹ The last term is the variation of the potential due to the presence of SBH inhomogeneity. Strictly speaking, Eq. (5) is not an exact solution to Poisson's equation because the change in the charge distribution near the edge of the depletion region, due to the presence of the SBH

inhomogeneity, has been ignored. However, for a rapidly fluctuating SBH or for any isolated variation of the SBH on a small lateral length scale, Eq. (5) gives a nearly perfect account of the potential close to the MS interface.^{15,16}

The most interesting form of SBH inhomogeneity is the presence of small regions with a low SBH, $\Phi_B^0 - \Delta$, embedded in an interface with an otherwise uniform high SBH, Φ_B^0 . The most convenient geometries to consider for the low-SBH regions are small circular patches and narrow semi-infinite strips, as shown schematically in Fig. 1. Numerical simulations have previously been performed for both geometries.^{19,21,22} For a low-SBH circular patch with radius R_0 , which is small compared with W , the potential at any point (ρ, z) , may be written down using Eq. (5). Along the z axis ($\rho=0$), the potential has an analytic form,

$$V(0, z) = V_{bb} \left[1 - \frac{z}{W} \right]^2 + V_n + V_a - \Delta \left[1 - \frac{z}{(z^2 + R_0^2)^{1/2}} \right]. \quad (6)$$

The excellent agreement between the potential obtained with the present dipole-layer approach and that obtained from solving Poisson's equation is shown in Fig. 2. Note that there are no fitting parameters for the curves drawn in Fig. 2. Details of the numerical simulations, using a program called PADRE (which produced the data shown in Fig. 2), are presented elsewhere.¹⁶ For a large Δ , or a small R_0 , the potential in front of the patch is obviously pinched-off. One notes that if the potential has a positive slope at small z , then it will go through a maximum before descending at large z to the value for a neutral semiconductor. Thus, the condition for pinch-off is obtained by differentiating Eq. (9) with respect to z and setting the derivative positive:

$$\frac{\Delta}{V_{bb}} > \frac{2R_0}{W}. \quad (7)$$

The condition set by (7) shows that potential pinch-off is

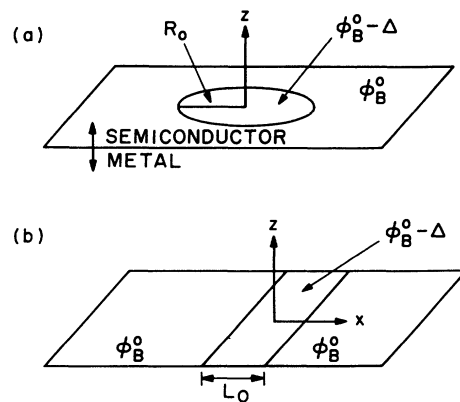


FIG. 1. Geometries and coordinates of examples used in the present work. (a) Circular patch, (b) narrow strip.

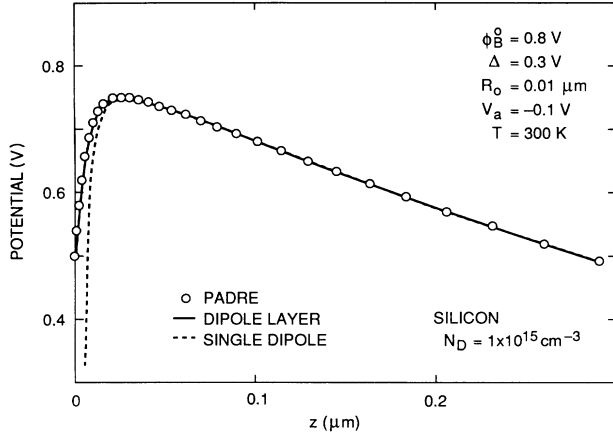


FIG. 2. Potential of the CBM, referenced to the FL, in front of a low-SBH circular patch. Circles represent a numerical solution (Ref. 16) to Poisson's equation. The solid curve is calculated from the analytical expression for a dipole layer, i.e., Eq. (6). The dashed curve is from the point-dipole approximation, Eq. (10).

most prominent when the semiconductor doping level is low. In Fig. 3, the potential close to the low-SBH patch is plotted to show that the smaller R_0 is, the easier it is for pinch-off to occur. The dependence of the potential on the applied bias, illustrated in Fig. 4, has a very significant impact on transport properties at inhomogeneities SBH junctions. The potential barrier between the semiconductor and the metal increases with forward bias. As will be discussed, this dependence of the potential on applied bias is the key to understanding a host of "anomalous" phenomena in I - V measurements. To first order, the potential does not depend on temperature.

For a semi-infinite strip of low-SBH, with a width of L_0 , the CBM potential in the space-charge region may be written down as [see coordinates shown in Fig. 1(b)]

$$V(x, y, z) = V_{bb} \left[1 - \frac{z}{W} \right]^2 + V_n + V_a - \frac{\Delta}{\pi} \tan^{-1} \left[\frac{|x| + L_0/2}{z} \right] + \frac{\Delta}{\pi} \tan^{-1} \left[\frac{|x| - L_0/2}{z} \right]. \quad (8)$$

The excellent agreement between the potential predicted by Eq. (8) and that obtained by numerically solving Poisson's equation has already been demonstrated.^{15,16} Lateral cross sections of the potential are shown in Fig. 5 to give a three-dimensional view of the potential contour near the saddle point. As before, the condition for pinch-off may be obtained:

$$\frac{\Delta}{V_{bb}} > \frac{\pi L_0}{2W}. \quad (9)$$

The validity of Eqs. (6)–(9) has been demonstrated extensively by recent numerical simulations.¹⁶

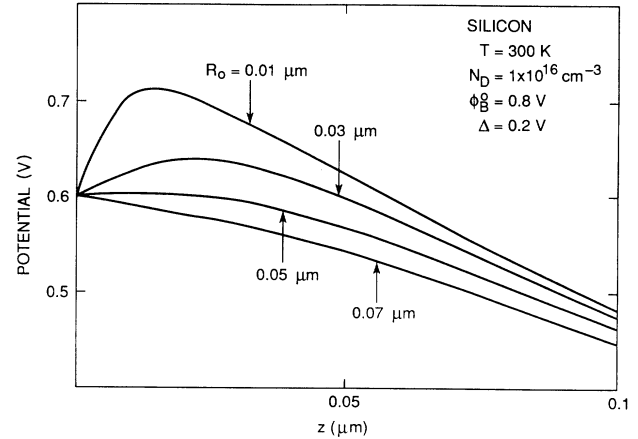


FIG. 3. CBM potentials along the z axis, calculated with Eq. (6), illustrating the influence of the radius of a low-SBH patch on potential pinch-off.

B. Point-dipole approximation

The approach described in the previous section gives a very accurate account of the electric potential in the presence of SBH inhomogeneity. When the dimension of low SBH patches or strips is small compared with the depletion length, one may further simplify the potential by replacing the spatially extended dipole patch or strip with a point dipole or a dipole line. Such a simplification gives a good approximation to the potential except very close to the patch or strip. This approach is quite adequate for an estimation of the expected I - V behavior from an inhomogeneous SBH distribution, because, as will be discussed, the most relevant potential for electron transport is that near the saddle point, some distance away from the MS interface.

For a circular patch with radius R_0 , the total dipole moment is $2\epsilon_s \Delta \pi R_0^2$. The potential around the patch, except near the core of the dipole, is given by

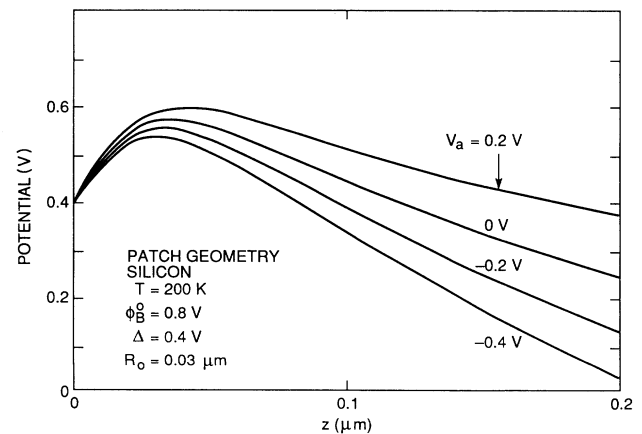


FIG. 4. The variation of potential with the applied bias for a low-SBH circular patch. Note that the saddle-point potential slowly rises with forward bias and slowly decreases with reverse bias.

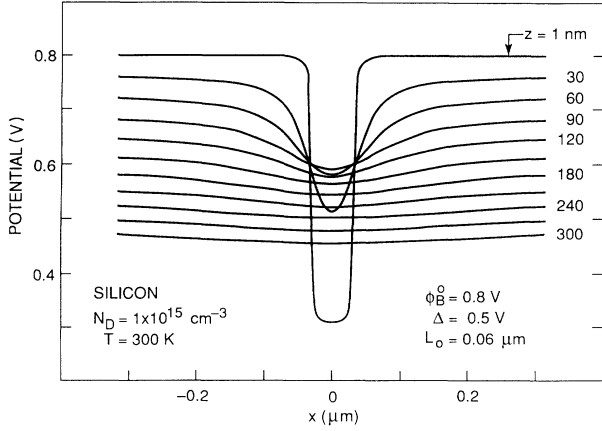


FIG. 5. CBM potential in front of a narrow low-SBH strip placed at $x=0$. Different slices of the potential, taken at different vertical distances (z) from the MS interface, illustrate the phenomenon of potential pinch-off.

$$V(\rho, z) = V_{bb} \left[1 - \frac{z}{W} \right]^2 + V_n + V_a - \frac{V_{bb} \Gamma^3 z W^2}{(\rho^2 + z^2)^{3/2}}, \quad (10)$$

where Γ is a dimensionless quantity that measures the “strength” of a given patch and is defined by

$$\Gamma^3 \equiv \frac{\Delta R_0^2}{2V_{bb} W^2} = \frac{\Delta R_0^2}{4\eta V_{bb}^2}, \quad (11)$$

where $\eta \equiv \epsilon_s / (qN_D)$. As shown in Fig. 2, the point-dipole approximation, Eq. (10), adequately describes the potential around the saddle point. The agreement is best when Δ is large and when $R_0 \ll W$. One notes that the present expression is not limited to low-SBH patches with a circular geometry, as Γ may be defined for any small patch with an irregular shape and/or a varying SBH by an integral:

$$\Gamma^3 \equiv \frac{-1}{4\pi\eta V_{bb}^2} \int_{\text{patch}} \delta(x_1, y_1) dx_1 dy_1. \quad (11a)$$

Because the point-dipole approximation lumps the effect of a dipole patch with a finite size into a point source, it

errs on slightly overestimating the depth of the potential “valley” at the saddle point and slightly underestimating the valley width.

When pinch-off occurs, the location of the saddle point, at $(0, z_0)$, may be obtained by differentiating Eq. (10) along the z axis and setting the derivative to zero. When $\Gamma \ll 1$, z_0 is found to be, approximately,

$$z_0 \approx W\Gamma, \quad (12)$$

and the saddle-point potential is

$$V_{\text{saddle}}^{\text{patch}} = V(0, z_0) \approx V_{bb}(1 - 3\Gamma) + V_n + V_a. \quad (13)$$

This represents the minimum potential barrier separating the low-SBH patch from the neutral semiconductor.

The dipole layer due to a semi-infinite strip with a width L_0 may be approximated by a “dipole line” with an infinitesimal width. The dipole moment per unit length is $2\epsilon_s \Delta L_0$, and the potential may be written down as follows:

$$V(x, y, z) = V_{bb} \left[1 - \frac{z}{W} \right]^2 + V_n + V_a - \frac{2V_{bb} \Omega^2 Wz}{x^2 + z^2}, \quad (14)$$

where Ω is a dimensionless quantity that measures the strength of the strip, defined in Table I. Using procedures similar to those described above, the location and the potential of the saddle point may also be found for the strip geometry (Table I).

III. ELECTRON TRANSPORT

A. An isolated region with a low SBH

With a knowledge of the electric potential around the saddle point, the current flowing to and from a low-SBH patch may now be evaluated. However, it should be recognized that the current transport over even a homogeneous SB is not yet fully understood. Experimental results tend to agree more closely with predictions of the thermionic emission theory than the diffusion theory. Note that existing theories have regarded the emission process as occurring at the highest point of the potential barrier. In the case of a (uniform) SBH that is lowered by

TABLE I. Electron transport at an isolated low-SBH region with a local SBH of $\Phi_B^0 - \Delta$, surrounded by regions with a SBH of Φ_B^0 .

Geometry	Circular patch	Semi-infinite strip
Dimension	Radius = R_0	Width = L_0 , length = $L_{\text{strip}} \gg L_0$
Region parameter	$\gamma = 3(\Delta R_0^2 / 4)^{1/3}$	$\omega = 2(\sqrt{2}L_0 \Delta / \pi)^{1/2}$
Space-charge parameter	$\Gamma = (R_0^2 \Delta / 2W^2 V_{bb})^{1/3}$	$\Omega = (L_0 \Delta / 2\pi W V_{bb})^{1/2}$
Saddle-point position	$(\rho=0, z=\Gamma W)$	$(0, y, z=\Omega W)$
Effective area	$A_{\text{eff}} = (4\pi\gamma/3\beta)(\eta/V_{bb})^{2/3} = (4/3)\pi\lambda_D^2 \Gamma$	$A_{\text{eff}} = (\pi\omega/\beta)^{1/2}(\eta/V_{bb})^{3/8} L_{\text{strip}}/2 = \sqrt{\pi}\Omega\lambda_D L_{\text{strip}}$
Effective SBH	$\Phi_{\text{eff}} = \Phi_B^0 - 3\Gamma V_{bb} = \Phi_B^0 - \gamma(V_{bb}/\eta)^{1/3}$	$\Phi_{\text{eff}} = \Phi_B^0 - 4\Omega V_{bb} = \Phi_B^0 - \omega(V_{bb}/\eta)^{1/4}$
Ideality factor	$n \approx 1 + \Gamma = 1 + \gamma\eta^{-1/3} V_{bb}^{-2/3} / 3$	$n \approx 1 + \Omega = 1 + \omega\eta^{-1/4} V_{bb}^{-3/4} / 4$

image force, thermionic emission occurs within the semiconductor and not directly at the MS interface. Such a theory obviously can be applied to the present situation with little modification. In the thermionic emission theory, the majority-carrier quasi-Fermi level is assumed to be uniform throughout the semiconductor, and the flux of electrons (holes) over a potential barrier of Φ (referenced to the majority-carrier quasi-Fermi level) is

$$J = \int_{\Phi}^{\infty} q v_z dn = A^* T^2 \exp(-\beta\Phi) . \quad (15)$$

In principle, electron transport across real MS interfaces depends on the band structures and may be both system specific and even region specific. In the present discussion, band effects will be ignored and a unique Richardson's constant is assumed to be applicable to all areas of the MS interface. For an inhomogeneous SB, the Φ in Eq. (15) may be identified as the local (laterally varying) CBM potential minus V_a . Ignoring the contribution from minority carrier, the total current is a sum of the current density J over the area. We shall first consider the case of a low-SBH patch, the potential of which is given by Eq. (10). The lateral distribution of potential around the saddle point may be expanded in a power series with respect to the radial coordinate ρ :

$$V(\rho, z_0) = V_{\text{saddle}}^{\text{patch}} + \frac{3\rho^2}{4\lambda_D^2 \Gamma} + \dots \quad (16)$$

for small ρ and $z_0 = \Gamma W$, where λ_D is the Debye length of the semiconductor, $\lambda_D = (\eta/\beta)^{1/2}$. One may neglect the higher-order terms and assume the potential at the saddle point to have a parabolic form. The total current at a SB junction at any bias may be thought of as consisting of two components, one flowing in the forward direction and one flowing in the reverse direction. Applying the thermionic emission theory, the current flowing in the forward direction over the barrier may be integrated:

$$\begin{aligned} I_{\text{patch}}^F &\approx A^* T^2 \exp(-\beta V_n - \beta V_{\text{bb}} + 3\beta \Gamma V_{\text{bb}}) \\ &\times \int_{\rho=0}^{\infty} \exp\left[-\frac{3\rho^2}{4\lambda_D^2 \Gamma}\right] 2\pi\rho d\rho \\ &= A^* T^2 \left[\frac{4\pi\gamma\eta^{2/3}}{9\beta V_{\text{bb}}^{2/3}} \right] \exp\left[-\beta\Phi_B^0 + \frac{\beta\gamma V_{\text{bb}}^{1/3}}{\eta^{1/3}}\right] \\ &\times \exp(\beta V_a) , \end{aligned} \quad (17)$$

where γ is a constant related to the patch characteristics, defined in Table I. One notes that γ is a true parameter of the MS interface inhomogeneity, while Γ is a parameter that depends on the doping level of the semiconductor, the applied bias, and even the temperature, slightly. Γ is a useful parameter because it is dimensionless and it measures the effect of SBH inhomogeneity on the space-charge region. The reverse current exactly balances the forward current at zero bias. Therefore, the net current may be written as follows:

$$\begin{aligned} I_{\text{patch}} &\approx A^* T^2 \left[\frac{4\pi\gamma\eta^{2/3}}{9\beta V_{\text{bb}}^{2/3}} \right] \exp\left[-\beta\Phi_B^0 + \frac{\beta\gamma V_{\text{bb}}^{1/3}}{\eta^{1/3}}\right] \\ &\times [\exp(\beta V_a) - 1] . \end{aligned} \quad (18)$$

A comparison of Eq. (18) with the usual expression for junction current from the thermionic emission theory, Eqs. (1) and (2), shows that a low-SBH patch may be considered as having an effective SBH, Φ_{eff} , and an effective area, A_{eff} , as defined in Table I. The effective SBH is simply the potential at the saddle point. Since V_{bb} decreases linearly with V_a , the applied bias voltage affects the current through both the usual exponential factor and the variation of Φ_{eff} with V_{bb} . With an increasing forward bias, the Φ_{eff} increases slowly (cf. Fig. 4). This dependence of the potential barrier on the applied bias leads to an ideality factor that is greater than 1. Differentiating the logarithm of the forward-biased current with respect to applied voltage shows that the ideality factor is

$$n = \beta \left[\frac{\partial \ln(I)}{\partial V_a} \right]^{-1} \approx 1 + \Gamma = 1 + \frac{\gamma}{3\eta^{1/3} V_{\text{bb}}^{2/3}} . \quad (19)$$

Because Γ increases slowly as the applied forward bias increases, there is a slight curvature to such a component of the current. Equation (19) and Table I show that the lower Φ_{eff} of a patch is, the larger is its ideality factor. The ideality factor and the effective SBH do not have an explicit dependence on temperature. As the doping level increases (η decreases), Φ_{eff} decreases and the ideality factor increases. The current density near the saddle point is much larger than the average current density. The Ohmic effect for a small low-SBH patch may be approximated by a spreading resistance for a disc²³ with an area equal to A_{eff} . Parameters governing the current flowing to a low-SBH strip, estimated using procedures similar to those described for a circular patch, are summarized in Table I. The validity of the expressions for electron transport, Table I, has been demonstrated recently by numerical simulations.¹⁶

B. SB diodes consisting of many low-SBH regions

The equations derived in the present work show that the current flowing across an inhomogeneous SB is indeed expressible in a sum similar to that shown in Eq. (3). However, the individual Φ_i and A_i should be replaced by their "effective" counterparts, $\Phi_{\text{eff},i}$ and $A_{\text{eff},i}$, respectively. Thus, the total junction current is a sum of currents flowing in each individual region,

$$I(V_a) = A^* T^2 [\exp(\beta V_a) - 1] \sum_i A_{\text{eff},i} \exp(-\beta\Phi_{\text{eff},i}) . \quad (20)$$

Note that the difference between Eqs. (20) and (3) is that $A_{\text{eff},i}$'s and $\Phi_{\text{eff},i}$'s depend on the applied bias, while A_i 's and Φ_i 's in Eq. (3) do not. Only when the low-SBH regions are not pinched-off does one revert to the parallel conduction model.¹⁸ Since patches and/or strips with low effective SBH's strongly affect the current transport

through a SB, the observed I - V behavior from a diode depends very much on the distribution of SBH's within the diode. The total current of an inhomogeneous SB diode may exhibit a variety of interesting behaviors. In this section, the expected behavior of the junction current from an inhomogeneous SB diode will be illustrated by way of examples.

1. Sharply distributed low-SBH patches and/or strips

When a low density of patches c_1 , with almost identical γ 's ($\gamma = \gamma_0$) are present in a SBH diode, the junction current is described by a small number of parameters. Low-SBH patches are assumed to be well separated from one another, hence the current flowing in each individual patch is not affected by the presence of other patches. Such an approach is analogous to a dilute solution treatment.²⁴ The total current flowing in the SB may be written down as

$$I_{\text{total}} = AA^*T^2 \exp(-\beta\Phi_B^0) [\exp(\beta V_a) - 1] \times \left[1 + \frac{4c_1\pi\eta^{2/3}\gamma_0}{9\beta V_{\text{bb}}^{2/3}} \exp\left(\frac{\beta\gamma_0 V_{\text{bb}}^{1/3}}{\eta^{1/3}}\right) \right]. \quad (21)$$

A similar expression may be obtained for the current flowing in a diode which contains low-SBH strips.

The total junction current is made up of two components, one of which is that characteristic of a diode with a SBH of Φ_B^0 and an area of A , represented by the numeral 1 in the second line of Eq. (21). The other is governed by the saddle-point potential, $\Phi_B^0 - \gamma_0 V_{\text{bb}}^{1/3} \eta^{-1/3}$, of the low-SBH patches. Depending on parameters such as the doping level, γ_0 , and c_1 , the diode current predicted by Eq. (21) may show a variety of behaviors. For example, a set of I - V characteristics, calculated for a SB diode that includes a single low-SBH patch, is shown in Fig. 6. At high temperatures, the junction current is dominated by thermionic emitted transport over the uniform SBH and displays near unity ideality factor. At low temperatures, the exponential term on the second line of Eq. (21) becomes much larger than 1, and the low-SBH patches dominate at small bias and the ideality factor is larger than 1. As mentioned earlier, the current density near a low-SBH patch may be orders of magnitude higher than the average current density and the Ohmic effect may be significant even at moderate forward bias. This is the reason for plateaulike sections in the I - V characteristic, as shown in Fig. 6. The two components of current may be deconvoluted at low temperatures.

When c_1 and/or γ_0 are large, the junction current may be dominated by the low-SBH patches at all practical bias and temperature ranges. Calculated I - V traces of such a diode, as shown in Fig. 7, display a slight curvature that originates from the dependence of Φ_{eff} on V_{bb} (cf. Table I). As a consequence of this curvature, the ideality factor and the saturation current deduced from any I - V trace depend on the bias range for which the linear fit is made. If a narrow *constant bias range* is used, the deduced ideality factors do not have a strong dependence on temperature. However, experimental I - V data are usually record-

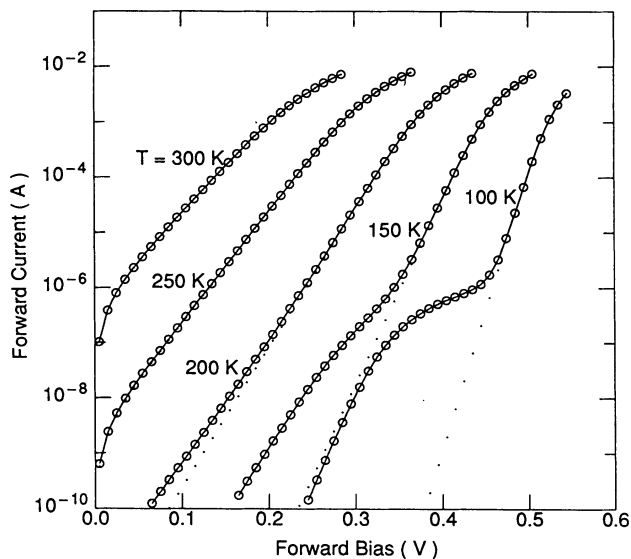


FIG. 6. Calculated forward current-voltage characteristics from a SB diode with an area of $4 \times 10^{-3} \text{ cm}^2$ and a temperature-independent Φ_B^0 of 0.65 V , which contains a low-SBH patch with a γ of $8 \times 10^{-4} \text{ cm}^{2/3}$. To calculate the series resistance and the spreading resistance, the semiconductor is assumed to be a $100\text{-}\mu\text{m}$ -thick layer of n -type Si, $1 \times 10^{15} \text{ cm}^{-3}$ doped.

ed, and therefore analyzed, within a *fixed current range*. When the calculated I - V traces of Fig 7 are analyzed within a narrow constant current range, as indicated by the dotted lines, the ideality factor is found to vary with temperature. Figures 6 and 7 are just two examples of the many different I - V behaviors that may be expected from low-SBH patch(es) with a single γ .

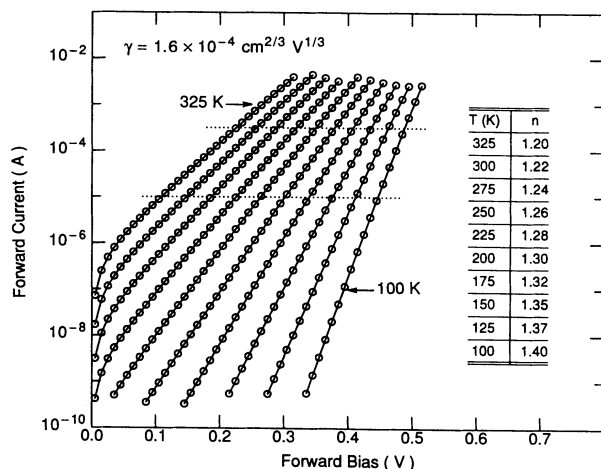


FIG. 7. I - V traces, calculated with Eq. (21), of a Si SB diode that contains a large number of low-SBH patches with a unique γ . $\Phi_B^0 = 0.8 \text{ V}$, $\gamma_0 = 1.6 \times 10^{-4} \text{ cm}^{2/3} \text{ V}^{1/3}$, and $N_D = 1 \times 10^{17} \text{ cm}^{-3}$. The SBH distribution is assumed to be independent of temperature. Series resistance, which is included in the calculation, has a negligible effect on the I - V characteristic. Ideality factors are deduced in a current range of $1 \times 10^{-5} - 3 \times 10^{-4} \text{ A}$.

2. Broad distribution of SBH variation

At a real MS interface, SBH variations are likely to occur in a variety of shapes and spatial frequencies. Consider the case of a SB diode with a constant SBH, Φ_B^0 , everywhere at the MS interface except at a few isolated small patches that have a lower SBH. One may imagine that there are an equal number of patches and/or strips present with higher-than-average SBH's to make the overall average of the SBH unchanged at Φ_B^0 . The patches and/or strips with a higher-than-average SBH contribute little to electron transport, and may be ignored in the present analysis. With the assumption of a statistical distribution of the patch or strip characteristics, it may be shown (see the Appendix) that the total junction current is approximately given by

$$I_{\text{total}} = A * AT^2 \exp(-\beta\Phi_B^0) [\exp(\beta V_a) - 1] \times [1 + f(V_{\text{bb}}) \exp(\beta^2 \kappa V_{\text{bb}}^\xi)], \quad (22)$$

where the constants ξ and κ and the slowly varying function f are defined in Table II.

The current in Eq. (22) is made up of two components: one being the current over the entire diode, which has a uniform SBH of Φ_B^0 , the other being an additional current due to the presence of the low-SBH patches and/or strips. The combined effect of all the low-SBH regions is as if there were a big low-SBH region in the diode with an effective area of (Af) and an effective SBH of

$$\Phi_{\text{eff}} = \Phi_B^0 - \beta \kappa V_{\text{bb}}^\xi. \quad (23)$$

Even though the effective SBH of each individual patch is roughly temperature independent, put together they may be represented by a temperature-dependent effective SBH. This leads to some very interesting temperature dependences of the junction current. Examples of I - V traces, calculated with Eq. (22), are shown in Fig. 8 for a diode whose total current is dominated by low-SBH patches. The ideality factors of the I - V traces have a much stronger dependence on temperature than those from diodes with a sharp distribution of patches (Fig. 7) because of their explicit dependence on temperature:

$$n_{\text{tot}} \approx 1 + \xi \beta \kappa V_{\text{bb}}^{\xi-1}. \quad (24)$$

However, it may be seen that the dependence of the overall ideality factor on bias ($\propto V_{\text{bb}}^{-1/3}$ in the patch geometry) is much weaker than that observed for each individual patch [$\propto V_{\text{bb}}^{-2/3}$, cf. Eq. (19)]. Within a range of

TABLE II. Parameters for electron transport at an inhomogeneous SB with a broad distribution of SBH's.

Parameter	Patch	Strip
ξ	$\frac{2}{3}$	$\frac{1}{2}$
κ	$\frac{\sigma_1^2}{2\eta^{2/3}}$	$\frac{\sigma_2^2}{2\eta^{1/2}}$
$f(\beta, V_{\text{bb}})$	$\frac{8c_1\sigma_1^2\pi\eta^{1/3}}{9V_{\text{bb}}^{1/3}}$	$\frac{c_2\pi\sigma_2^{3/2}\sqrt{\beta}\eta^{1/8}L_{\text{strip}}}{1.46V_{\text{bb}}^{1/8}}$

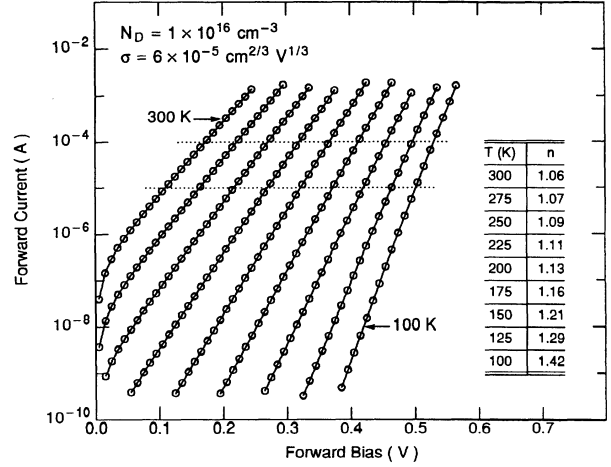


FIG. 8. I - V traces, calculated with Eq. (22), of an inhomogeneous Si SB diode with the following parameters: $N_D = 1 \times 10^{16} \text{ cm}^{-3}$, $\sigma_1 = 6 \times 10^{-5} \text{ cm}^{2/3} \text{ V}^{1/3}$, and $\Phi_B^0 = 0.8 \text{ V}$. Ideality factors and saturation currents are deduced in a current range of $1 \times 10^{-5} - 1 \times 10^{-4} \text{ A}$.

a few decades of the current, the curvature of the I - V trace is hardly noticeable, as illustrated in Fig. 8. Within one given SB diode, the variation of SBH may occur in more than one possible form of SBH inhomogeneity. To further generalize, one may consider the exponent ξ in Eq. (22) to be a measure of the geometry of the SBH variation, which may be empirically determined by fitting the functional form of the experimentally observed currents.

IV. SBH ANOMALIES EXPLAINED BY SBH INHOMOGENEITY

Experimentally observed behaviors from real SB's often show considerable departures from that expected of ideal MS interfaces.^{1,25,26} As will be shown, all of the common nonideal, or anomalous, phenomena may be explained by SBH inhomogeneity. It is also pointed out that existing explanations of these anomalies, mostly based on interface states, are not consistent with all the experimental results.

A. Leakages and edge-related currents

Experimentally observed I - V curves have frequently been analyzed²⁷ and shown to be comprised of two or more components of current. At small biases, the forward current is sometimes dominated by a "soft," or "leaky," component that leads to both a curvature in the I - V curve and tangential slopes corresponding to ideality factors much in excess of 1. As bias increases, the I - V relationship becomes semilogarithmic with an ideality factor not far from unity, e.g., low-temperature traces shown in Fig. 6. It is customary to attribute the linear portion of the I - V curve to the main conduction mechanism, e.g., thermionic emission over the SB, and the leakage current at low biases to a different mechanism. Generation and recombination in the space-charge region,²⁸ interface states,²⁹ and edge-related conduction^{30,31} are the mechanisms most frequently thought to lead to the leakage

currents. As has been pointed out,³² the attribution of leakage current to interface states²⁹ is not consistent with experimentally observed I - V characteristics. Because edge-related currents scale with the peripheral length of the diode, and not with the area of the diode, they may be unambiguously identified by using diodes with different sizes.^{30,33} Edge-related currents are often thought to be due to a larger electric field at the diode edges, which leads to increased tunneling and/or increased generation or recombination.²⁸ However, detailed analysis often showed that edge-related currents have ideality factors similar to,³⁰ or smaller than,^{33,34} those associated with the center portions of the diodes. These observations indicate that edge-related currents should not be indiscriminately attributed to the generation-recombination process. When the leakage current is not clearly related to edges, the generation-recombination process is still the explanation most commonly invoked. However, the fact that leakage currents were observed to be clearly dominating in some diodes and completely missing in other diodes on the same sample³³ seems inconsistent with the explanation based on generation-recombination centers.

The present work shows that experimentally observed leakage currents are consistent with SBH inhomogeneity. The presence of a few large low-SBH regions (with their large γ 's and, hence, large ideality factors) in the SB diode can certainly lead to the appearance of a leaky component in the junction current, as illustrated in Fig. 6. The small slope of this current (high ideality factor) and effects due to series resistance limit the predominance of this leakage component to small forward biases. Because of a lower effective SBH, the presence of even a single low-SBH region can lead to the appearance of leakage current. Experimentally observed diode-to-diode variations of the leakage current are in much better agreement with isolated "leakage spots" due to low local SBH than with a distribution of recombination centers in the space-charge region. The existence of a current component that is proportional to the perimeter of the diode is also in good agreement with SBH inhomogeneity. A low-SBH patch is less effectively pinched-off when it is situated in close proximity (on the order of the depletion width) to the edge than when it is in the central portion of a diode, as has been clearly demonstrated by computer simulations.¹⁶ When a SB diode contains a uniform distribution of low-SBH patches, the number of patches that are found near the edges is proportional to the perimeter. Depending on the exact nature of the inhomogeneity, the edge-related current may have an ideality factor that is either larger or smaller than that associated with the planar part of the diode. Clearly, leakage and edge-related currents are all consistent with SBH inhomogeneity.

B. Greater-than-unity ideality factors

Experimentally observed I - V characteristics are almost always semilogarithmic, in agreement with the thermionic emission theory. However, the slopes of such traces often differ from the theoretical predictions, which necessitated the inclusion of the empirical ideality factor³⁵ in the description of the junction current, Eq. (1). An ideality

factor greater than 1 has no direct explanation within the thermionic emission theory, and is generally attributed to a SBH that is bias dependent. Image force lowering,³⁶ generation-recombination, interface states,^{37,38} and thermionic field emission (TFE) (Ref. 39) have all been discussed as possible mechanisms that could lead to a greater-than-unity ideality factor. Since the image-force lowering and the TFE may be calculated and the generation-recombination contribution can be distinguished experimentally, the maximum ideality factor due to these mechanisms may be accurately estimated. Observed ideality factors often far exceed these estimates, prompting the proposal that interface states are a main origin of greater-than-unity ideality factors.

There are two entirely different proposals to explain the nonideal behavior based on interface states: the interface-layer (the tunnel MIS diode) approach³⁷ and the intimate MIGS (negative-charge) approach.^{38,40} Greater-than-unity ideality factors are not necessarily associated with an interface layer because they are often observed at annealed, intimate, MS interfaces. Generally speaking, the interpretation based on an interface layer is not consistent with both the bias dependence and the work-function dependence of the SBH's, as already pointed out.⁴¹ At intimate SB interfaces, the upward bending of the semiconductor bands near the MS interface due to the spatial extension of the (negative) charge is the mechanism by which ideality factors are explained with the interface states models.^{38,40} However, since the short-range band bending is independent of the semiconductor doping type, it may be used to explain only the ideality factor on one type of semiconductor. Experimental results show large ideality factors on both n - and p -type semiconductors, in disagreement with the negative-charge mechanism. In addition, the ideality factors are often found to vary significantly with processing, or from diode to diode on the same sample, while the SBH's are essentially the same. These results are difficult to explain with interface states, because the interface states are assumed to decide both the magnitude of the SBH and the ideality factor of a SB diode.

The bias dependence of the effective SBH's (saddle-point potentials) of inhomogeneous SB's can explain all the observed behavior of the ideality factor. Since the currents of SB diodes are often dominated by low-SBH patches, greater-than-unity ideality factors are routinely observed. When the doping level increases (η decreases), the Φ_{eff} of a low-SBH patch with a fixed γ decreases and its ideality factor increases, in good agreement with experimental observations. The diode-to-diode variation of the ideality factor and the dependence on processing are also consistent with variations in the distribution of local SBH in the diodes under study. High-quality single-crystal silicide-Si interfaces usually display ideality factors very close to unity³² because of the homogeneity of the interface structure and the SBH. Deliberate introduction of SBH inhomogeneity has been shown to lead to large ideality factors.¹¹ Since the ideality factor is simply a manifestation of the SBH uniformity, it is not surprising that it may be improved by improving the uniformity of the layer, which presumably also leads to a more uni-

form interface structure.⁴² Nor should one find it odd that the ideality factor is the largest when the layer is the most nonuniform.⁴³ Since the vast majority of polycrystalline MS interfaces display ideality factors significantly greater than 1, the SBH's of most MS interfaces are likely inhomogeneous.

C. The T_0 anomaly

Many different temperature dependences of the ideality factor have been observed experimentally. Most frequently, the ideality factor of a diode increases when the sample temperature is lowered. At many MS interfaces, the deduced SBH and ideality factors are found to vary with the measurement temperature in a fashion generally known as the " T_0 anomaly."^{44,45} Such a phenomenon has been observed from all types of SB's, on elemental semiconductors⁴⁵ and compound semiconductors^{44,46} alike. A diode is said to display the T_0 effect if its junction current may be expressed as

$$I_{\text{total}} = A^{**} AT^2 \exp \left[-\frac{q\Phi_B}{k_B(T+T_0)} \right] \times \left[\exp \left[\frac{qV_a}{k_B(T+T_0)} \right] - 1 \right], \quad (25)$$

where T_0 is a constant. Demonstration of the T_0 effect is usually accomplished by plotting $nk_B T$ (the inverse slope of an I - V curve) against $k_B T$ and observing a straight line, with a slope of unity, which does not extrapolate through the origin, as line 3 of Fig. 9. Concurrently, by

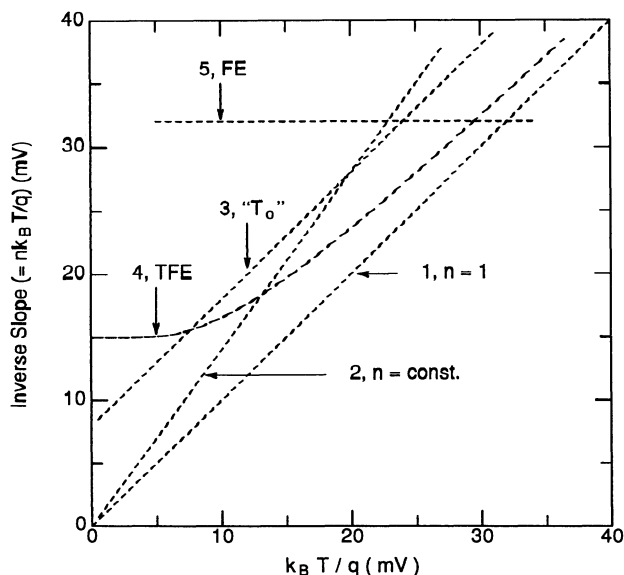


FIG. 9. Plot of inverse slope (V_0) vs $k_B T/q$, showing the five basic categories of the temperature dependence of the ideality factor. Line 1 is an ideal SB that follows the prediction of thermionic emission theory. Line 2 shows a temperature-independent, greater-than-unity ideality factor. Line 3 displays the T_0 effect. Lines 4 and 5 represent the behaviors when conduction is dominated by TFE and FE, respectively. [Replotted from A. N. Saxena (Ref. 45).]

changing the abscissa of the Richardson plot from $1/T$ to $1/nT$, a straight line should be observed in cases displaying the T_0 anomaly. Until recently, the T_0 anomaly has been ascribed to an exponential distribution of the density of interface states.^{47,48} However, such a model depends on the presence of an interface layer,⁴⁸ and hence is not consistent with the observation of the T_0 anomaly at intimate MS contacts.^{49,50} The facts that the measured T_0 varies significantly among similarly fabricated diodes⁵¹ and that T_0 may be locally varying in a large diode⁵² suggest that the T_0 anomaly is not directly related to the formation mechanism of the SBH.

SBH inhomogeneities offer an excellent explanation of the T_0 anomaly. As the temperature is lowered, the current of an inhomogeneous SB displays two trends, either of which can lead to the T_0 effect. First, as shown in Fig. 7, an increase in the bias results in an increase in the measured ideality factor. Secondly, the current of a random SB diode that contains low-SBH regions with a distribution of γ 's is described by Eq. (22), which, as shown in the Appendix, may be expressed phenomenologically in a form identical to Eq. (25). Therefore, when the temperature is lowered, the junction current is dominated by fewer low-SBH regions with lower effective SBH's and larger ideality factors. As an example, the inverse slope, in an I - V simulation, of a SB diode with low-SBH patches of just two distinct γ 's is plotted in Fig. 10 to illustrate the origin of the T_0 mystery. The empirical constant T_0 , which depends on how the ideality factor is evaluated experimentally, is related to the doping level and the distribution of the SBH (e.g., see the Appendix). Since the fluctuation of SBH likely varies for different diodes, the inconsistency of the apparent T_0 's (Refs. 51 and 52) and the doping dependence⁵³ are all naturally explained.

D. Other temperature dependences of the ideality factor

It is usually assumed that a study of the dependence of the ideality factor on temperature can reveal the conduction mechanism of a particular SB diode. The T_0 phenomenon is only one (line 3) of the five distinct temperature dependences according to the original categorization by Saxena,⁴⁵ shown in Fig. 9. A temperature-independent, large ideality factor (line 2) has often been observed experimentally, as has a dependence (line 4) that is usually attributed to a domination of the conduction mechanism by TFE.³⁹ However, temperature dependences similar to line 4 have often been observed under experimental conditions where tunneling should be negligible.⁵⁴ The ideality factor of an inhomogeneous SB diode with a wide distribution of low-SBH patches may increase at a rate even faster than the T_0 effect when the temperature is lowered. This effect is significantly magnified when series resistance influences the current flowing in the low-SBH patches. For example, calculated I - V curves from a composite SBH diode, under conditions where the series resistance effect is significant, are shown in Fig. 11(a). The composition of the total current is explicitly illustrated for two selected temperatures. The evaluated ideality factors are shown in Fig. 11(b),

which qualitatively reproduces the behavior usually attributed to the TFE mechanism. Thus, even though tunneling should dominate the electron conduction at heavily doped MS junctions, TFE is not necessarily the conduction mechanism whenever a dependence like that in Fig. 11(b) is observed. The temperature dependence of the ideality factor, by itself, does not provide a determination of the conduction mechanism.

Many temperature dependences of the ideality factor have been experimentally observed, and are all consistent

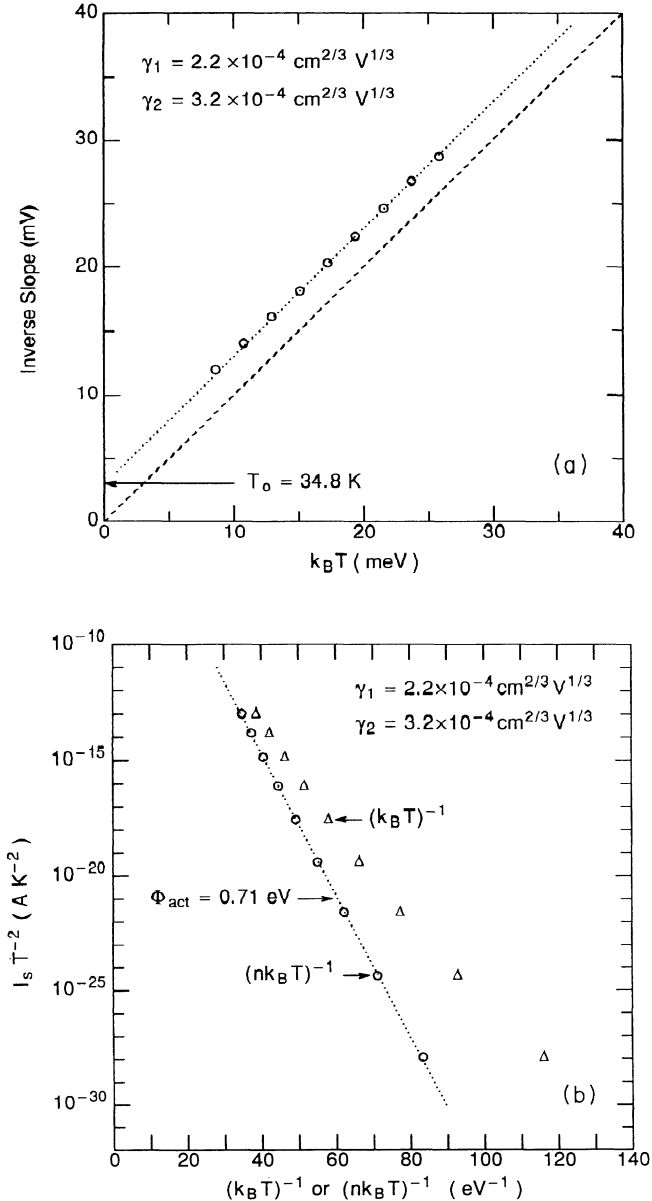


FIG. 10. I - V characteristics, calculated with Eq. (20), of an inhomogeneous SB diode, with a $\Phi_B^0 = 0.8$ V and an area of 4×10^{-3} cm². Low-SBH patches with γ 's of 3.2×10^{-4} cm^{2/3} V^{1/3} ($\times 800$) and 2.2×10^{-4} cm^{2/3} V^{1/3} ($\times 800000$) are included. Ideality factors and saturation currents are deduced in a current range of 3×10^{-7} – 3×10^{-6} A. (a) Inverse slope plot, (b) regular and modified Richardson plot of the saturation current. The semiconductor is Si with an N_D of 1×10^{16} cm⁻³.

with SBH inhomogeneity.¹⁶ When Φ_{eff} 's are low, only a small change in the bias is needed when the temperature is varied (in order) to maintain a constant current level. Therefore, a temperature-independent, greater-than-unity ideality factor, frequently observed at SB diodes with small SBH's,⁴⁹ is consistent with a SB diode whose current transport is dominated by low-SBH regions. A

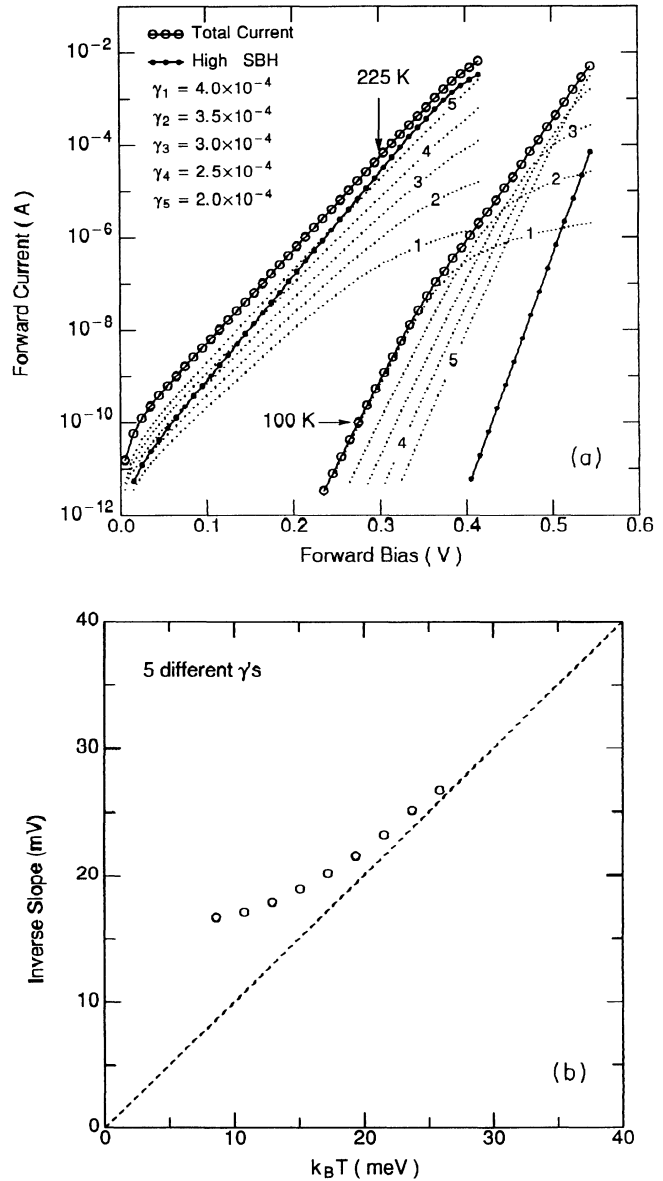


FIG. 11. I - V characteristics of an inhomogeneous Si SB diode ($N_D = 1 \times 10^{16}$ cm⁻³) with a Φ_B^0 of 0.7 V and an area of 4×10^{-3} cm². The following low-SBH patches are included: $\gamma = 4 \times 10^{-4}$ ($\times 1$), 3.5×10^{-4} ($\times 20$), 3×10^{-4} ($\times 400$), 2.5×10^{-4} ($\times 8000$), and 2×10^{-4} cm^{2/3} V^{1/3} ($\times 160000$). Ideality factors and saturation currents are deduced in a current range of 3×10^{-6} – 3×10^{-4} A. (a) Breakdown of the total current into individual components for two different temperatures, (b) inverse slope of the total current. The displayed temperature dependence of the ideality factor is similar to that usually ascribed in TFE.

decrease of the ideality factor with cooling⁵⁵ is consistent with the presence of general SBH inhomogeneity about some mean SBH and, in addition, a small number of low-SBH regions that are large enough that they are not pinched-off, as demonstrated by recent simulations.¹⁶ Frequently, the ideality factor of a SB diode is found to follow different behaviors at different temperature ranges,⁵⁰ i.e., switching between lines of Fig. 9. As the example of Fig. 6 shows, the junction current may be dominated by different components at different temperatures, leading to apparent switchovers between different dependences. Discussions in the last three sections show that the entire spectrum of widely different behaviors of the ideality factor can all be explained with SBH inhomogeneities.

E. "Soft" reverse characteristics

It is a universal observation that the current from any SB diode never truly saturates at large reverse bias. These "soft" reverse characteristics are observed even when the utmost care is taken to eliminate possible effects due to edges of the diode.³¹ A linear relationship is often observed by plotting the logarithm of the current against $V_{bb}^{1/4}$,^{28,56,57} in agreement with the functional dependence of the proposed image-force SBH lowering mechanism. However, the observed slopes from such plots often far exceed that predicted by the image-force mechanism alone.^{28,56,57} Andrews and Lepselter⁵⁸ proposed that, in addition to SBH lowering due to image-force, $\delta\Phi_{\text{image}}$, there is a SBH lowering which is proportional to E_{max} , the electric field, i.e.,

$$\begin{aligned} \delta\Phi &= \delta\Phi_{\text{image}} + \alpha E_{\text{max}} \\ &= \frac{1}{2} \left[\frac{2q^3 V_{bb} N_D}{\pi^2 \epsilon_s^3} \right]^{1/4} + \alpha \left[\frac{2q N_D V_{bb}}{\epsilon_s} \right]^{1/2}. \end{aligned} \quad (26)$$

This additional SBH lowering is thought to arise from the upward bending of the semiconductor band due to MIGS's (the negative charge model).^{3,40} In Eq. (26), the constant α is thought to be related to the density and depth of the interface states.⁴⁰ Experimental results in agreement with the prediction of this model have been observed in many studies.⁵⁸⁻⁶⁰ However, even though the functional form of many experimental reverse currents may be explained by this model, other consequences of this model have not been born out by experiments. For example, it is not clear why very different α 's are found for similar MS interfaces. Also, the proposed mechanism of SBH lowering is completely absent in some diodes.³⁶ As already discussed, the negative-charge mechanism allows SBH lowering for only one type of semiconductor. Experimental results^{58,60} indicated that the soft SB characteristics for many metals and/or silicides occurred with similar magnitudes on both *n*- and *p*-type semiconductors. Therefore, experimentally observed reverse characteristics at intimate MS interfaces are not entirely consistent with interface states.

Due to the limited range of available reverse bias, a reliable determination of the functional form of the current of any particular SB diode is difficult. In addition, the re-

verse currents of different diodes often show different behaviors. Therefore, even though Eq. (26) may account for the observed reverse current of some diodes, it is by no means the only lowering mechanism that may explain the experimental data. Any SBH-lowering mechanism that varies with the reverse bias more rapidly than $V_{bb}^{1/4}$ could lead to a satisfactory fit with the experimentally observed reverse currents. Presently, the reverse characteristics of an inhomogeneous SB are shown to depend critically on the actual variation of the SBH. From Eqs. (21) and (22), SBH lowerings proportional to the $\frac{1}{2}$ and $\frac{2}{3}$ powers of V_{bb} are all possible. At an inhomogeneous diode, the image-force-lowering mechanism may still apply to the high-SBH regions, but it does not apply to low-SBH regions that are already pinched-off. In Fig. 12, typical reverse currents from an inhomogeneous SB, which contains a distribution of low-SBH patches, are shown to give an excellent explanation of the experimentally observed reverse currents. At very large biases, currents based on SBH inhomogeneity fit the experimental data better than even the theoretical curves of Andrews and Lepselter.⁵⁸ The wide range of behaviors of reverse currents experimentally observed from various SB's suggests that the problem is complicated and that each specific diode may have its own individuality. Such a scenario is in complete accord with SBH inhomogeneity and is not easily reconciled with the interface state model.^{40,58}

F. Dependence of SBH on measurement technique

The SBH measured by the *I-V* technique, Φ_{I-V} , often decreases with increasing doping level, while the SBH measured by the *C-V* method, Φ_{C-V} , remains constant. Frequently, the SBH's depend on the technique of measurement, namely, Φ_{C-V} sometimes significantly exceeds Φ_{I-V} and the SBH derived from PR techniques, Φ_{PR} .⁶¹ Identical to the proposed explanations of the ideality fac-

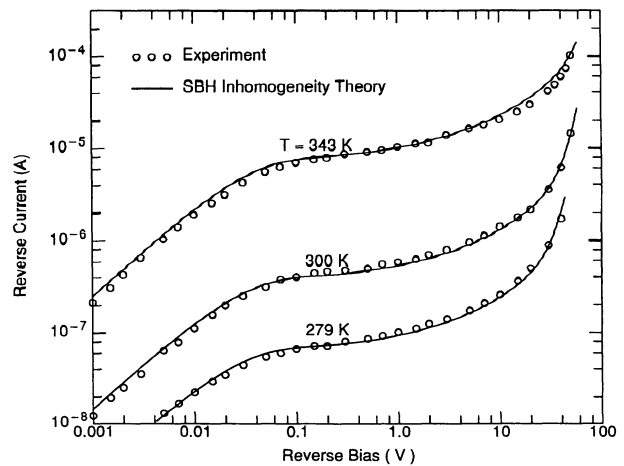


FIG. 12. Reverse characteristics (circles) of a ZrSi_2 Schottky diode experimentally observed by Andrews and Lepselter (Ref. 58). Solid lines are calculated currents of an inhomogeneous SB diode, which has a Φ_B^0 of 0.56 V and contains low-SBH patches with γ 's of $5.6 \times 10^{-5} \text{ cm}^{2/3} \text{ V}^{1/3}$ and $4 \times 10^{-5} \text{ cm}^{2/3} \text{ V}^{1/3}$.

tor, lowering of the SBH by image-force, interface states, and TFE have frequently been invoked to explain the doping-level dependence of Φ_{J-V} 's.^{38,62} While SBH investigations, especially those where the doping dependence of the SBH has been studied, have generally concentrated on *n*-type semiconductors, it is known that SBH lowerings on *p*-type semiconductors also routinely exceed that predicted by image force alone. Thus, it is clear that the observed doping dependence of moderately doped, intimate, SB contacts may not be attributed to interface states as previously thought. Rather, it is in agreement with the presence of SBH inhomogeneities.^{19,18,63-65} Current transport at inhomogeneous SB's is dominated by low-SBH patches, leading to the deduction by *I-V* and PR techniques of apparent SBH's that are lower than the arithmetic average of the entire diode. Since, under usual circumstances, the *C-V* technique yields an average SBH for the whole diode,¹⁵ the experimentally observed dependence of SBH on the technique of measurement is in good agreement with SBH inhomogeneity.

V. DISCUSSIONS

A. The issue of SBH inhomogeneity

It was clear, from the earliest SBH experiments on, that phenomena occurring at MS interface were always more complicated than the proposed theories and mechanisms could explain. Departures from theoretical predictions were observed more frequently than "ideal" behavior. These inconsistencies in experimental results are suggestive of interface electronic properties that are more complicated than the simple models that have thus far been proposed. Experimental results show that the chemical and physical properties of MS interfaces often vary with the material system, with differences in processing, or even from region to region on the same sample. In the light of the diversity of observed SBH behaviors, it is amazing that most SB investigations do not allow for the possibility that the SBH within one diode may vary. *A priori* there is no more reason to assume the SBH to be homogeneous than there is to assume that it is inhomogeneous. One may even argue that it makes more sense to start the treatment of SB junctions with a general theory of arbitrary SBH distribution than it is to immediately assume a uniform SBH. After all, a theory of inhomogeneous SB's may be easily applied to treat the homogeneous SB's as a special case, and, as we have seen, electron-transport theories of homogeneous SB's cannot be simply extended to treat inhomogeneous SB's. It should be kept in mind that the customary assumption of SBH inhomogeneity originates from convenience, rather than through scientific deduction.

Recently, the importance of understanding the SBH inhomogeneity issue is becoming increasingly apparent. Pioneering works in this area by Ohdomari, Freeouf, Bikbaev, Werner, and their colleagues have lead to a qualitative understanding of some behaviors from inhomogeneous SB's. For example, the important phenomenon of potential pinch-off has been numerically demonstrated by Freeouf *et al.*¹⁹ in two dimensions and by Bastys *et al.*²¹

in three dimensions. However, the coarse voltage steps and the effects due to series resistance have blurred the dependence of ideality factor on the dimension of the low-SBH strip or patch in previous calculations.^{19,21} Therefore, the connection between a large ideality factor and SBH inhomogeneities were not noted in these numerical studies.^{19,21} Without this connection, it was not obvious that SBH inhomogeneity is an issue that is relevant to the vast majority of SB's. A recent treatment⁶⁶ of this relationship did not address the lateral length scale of the inhomogeneity, and, as a result, failed to identify the true mechanism of the bias dependence of the SBH, namely, potential pinch-off. The present theory allows an analytical treatment of the potential and the electron transport at SB's with arbitrary SBH distributions. From a comparison of the simple expressions presently derived with experimental results reported in the literature, it is demonstrated that the vast majority of MS interfaces have inhomogeneous SBH's. Existing theories of electron transport, based on a uniform SBH, are not adequate for the interpretation of most experimental data, and should be replaced by the present general theory. The validity of the analytical expressions derived in this work has already been clearly demonstrated by a comparison with numerical solutions¹⁶ and a comparison with experimental results obtained from diodes with known inhomogeneity.¹¹

Direct evidence for inhomogeneity in the SBH's has been recognized.⁶⁷ Recently, exciting prospects of studying SBH variations on an atomic scale were offered by the invention of ballistic electron emission microscopy (BEEM).⁶⁸ However, since electrons have to reach the neutral semiconductor, the resolution of BEEM is limited by potential pinch-off in a fashion similar to any other *I-V* study, as recently pointed out.^{15,11} From the present discussion, it is clear that SBH inhomogeneity is a widespread phenomenon that affects the majority of SB's. The experimental data discussed in this work that demonstrate the presence of SBH inhomogeneities tend to be obtained on lightly doped semiconductors, which typically have a depletion region width on the order of 100–1000 nm. The observed potential pinch-off suggests that the length scale with which the SBH varies at such a MS interface is typically less than 100 nm. From the magnitude of the observed effects, it may be deduced that the local SBH may be modulating by as much as one-half the band gap for some of the diodes.

B. Interface states, Fermi-level pinning, and SB models

The validity of the present theory is independent of the formation mechanism of the SBH and the origin of SBH inhomogeneity. However, experimentally observed SBH inhomogeneities have certain implications on SB theories. For example, a homogeneous pinning of the FL, assumed in existing interface-states models,³⁻⁵ is not consistent with the present result. There is no question that interface-specific gap states are present at MS interfaces. However, there is little evidence to suggest that they lead to the formation of the SB in the fashion proposed by existing models.³⁻⁵ It has been a common practice for

SBH investigators to attribute changes in the electronic properties of the MS interface to changes in (laterally uniform) interface-state distributions. The present work and discussions elsewhere³² show that such an ascription of a host of anomalous SBH behaviors to interface states is unfounded. Clearly, the large fluctuation of the local SBH can only be explained by formation mechanisms that are dependent on the local specifics of the MS interface. In other words, proposed formation mechanisms, such as defects,⁶ MIGS,⁴ effective work function,⁶⁹ and chemical reactivity,⁷⁰ need to be broadened to address the issue of SBH inhomogeneity. Of course, the proposal of a structure-dependent interface dipole⁸ already explains SBH inhomogeneities very well.

In the light of the present evidence for SBH inhomogeneities in polycrystalline SB diodes, the very approach of concentrating only on the magnitudes of the experimental SBH's, in order to assess the validity of a SB theory, seems inappropriate. If a MS interface has an inhomogeneous SBH, then the SBH experimentally obtained from this interface is just an averaged value of some weighted distribution of different FL positions. Such an average does not necessarily have any physical significance. The true formation mechanism of the SB seems to be the one that determines the local FL position based on the local specifics of the MS interface. Due to the wide range of possible SBH distributions, it is not always possible to deconvolute the experimental results to obtain a complete profile of any given inhomogeneous MS interface. One has the additional difficulty that the present classical treatment breaks down in the presence of a rapidly varying field. It thus appears that the local SB mechanism is best studied in homogeneous MS systems. As mentioned earlier, recent results obtained from high-quality, epitaxial MS interfaces^{8,13,11,10,71} suggest that the formation of the SB depends on local specifics, such as the structure, of the MS interface.

VI. CONCLUSIONS

A simple approach to determine the potential and the current transport at MS interfaces with arbitrary SBH distributions is described. It is shown that, under usual experimental conditions, internal interactions among regions of different local SBH's cannot be neglected. Analytical expressions derived in the present work form the basis for understanding a host of experimental phenomena that presently have no, or only empirical, explanations. Specifically, it is shown that leakages, edge-related currents, greater-than-unity ideality factors, T_0 and other dependences of the ideality factor on temperature, soft reverse characteristics, and the dependence of the SBH on the measurement technique are all natural results of SBH inhomogeneity. This discovery suggests that the existence of SBH inhomogeneity is a much more common phenomenon than presently realized. Furthermore, it suggests that the mechanism responsible for SB formation depends on the local specifics of the MS interface.

ACKNOWLEDGMENTS

I would like to thank John Sullivan, Mark Pinto, and Jurgen Werner for discussions.

APPENDIX: SB DIODES WITH A DISTRIBUTION OF LOW-SBH REGIONS

1. Electron-transport equations

The density of patches with their parameter γ lying between γ and $\gamma + d\gamma$ is $N(\gamma)d\gamma$, and is assumed to have one-half of a Gaussian distribution:

$$N(\gamma) = \frac{\sqrt{2}c_1}{\sqrt{\pi}\sigma_1} \exp\left[-\frac{\gamma^2}{2\sigma_1^2}\right], \quad \gamma > 0, \\ N(\gamma) = 0, \quad \gamma < 0, \quad (\text{A1})$$

where σ_1 is the standard deviation and c_1 is the total density of patches. As before, low-SBH patches are assumed to be well separated from each other and hence do not interact with each other. Therefore, the total current at any given bias may be obtained by an integration over all the patches:

$$I_{\text{total}} = AA^*T^2 \exp(-\beta\Phi_B^0) [\exp(\beta V_a) - 1] \\ \times \left\{ \frac{4\sigma_1^2 \pi C_1 \eta^{1/3}}{9V_{\text{bb}}^{1/3}} \exp\left[\frac{\beta^2 \sigma_1^2 V_{\text{bb}}^{2/3}}{2\eta^{2/3}}\right] \right. \\ \left. \times \left[1 + \operatorname{erf}\left[\frac{\beta\sigma V_{\text{bb}}^{1/3}}{\sqrt{2}\eta^{1/3}}\right] \right] + 1 \right\}. \quad (\text{A2})$$

For usual values of temperature, doping level, etc., the numerical value of the error function is essentially 1. Therefore, a simple form of the junction current is arrived at:

$$I_{\text{total}} = A^*AT^2 \exp(-\beta\Phi_B^0) [\exp(\beta V_a) - 1] \\ \times [1 + f(\beta, V_{\text{bb}}) \exp(\beta^2 \kappa V_{\text{bb}}^\xi)], \quad (\text{A3})$$

where the function f , which varies slowly compared to the exponential function, and the constants κ and ξ are defined in Table II.

If a SB diode contains a random distribution of low-SBH strips, the junction may be evaluated using similar procedures. For the strip geometry, it turns out that the mathematics is simpler if a Γ distribution is assumed, i.e.,

$$N(\omega) = \frac{2c_2\sqrt{\omega}}{1.23(2\sigma_2^2)^{3/4}} \exp\left[-\frac{\omega^2}{2\sigma_2^2}\right] \quad (\text{A4})$$

for $\omega > 0$, where c_2 is the total density of strips and 1.23 is the numerical value of $\Gamma(\frac{3}{4})$. It may be shown that the total current is also expressible in a form identical to Eq. (A3), albeit with a set of differently defined parameters (Table II).

2. Temperature dependence of forward currents

In an actual SBH experiment, the forward current is fitted, over some finite range of forward bias, to the ther-

mionic emission theory with the form shown in Eq. (1). For a current described by Eq.(A3), the ideality factor is

$$n \approx 1 + \beta \xi \kappa V_{b0}^{\xi-1}, \quad (\text{A5})$$

and the saturation current is

$$\ln(I_s) = \ln(A A^* T^2 f) - \beta \Phi_B^0 + \beta^2 \kappa \xi V_{bi} V_{b0}^{\xi-1} + \beta^2 \kappa (1 - \xi) V_{b0}^{\xi}, \quad (\text{A6})$$

where V_{b0} is the band bending at the measurement bias, and V_{bi} is the built-in potential (band bending at zero bias). The weakly varying function f has been treated as a constant in such an analysis.

In the presence of SBH inhomogeneity, the deduced ideality factor and SBH obviously depend on the measurement temperature and on the choice of bias range in the analysis. If a *constant bias range* is used ($V_{bb} = V_{b0} \pm 3k_B T/q$), it may be shown that the current is given by the following phenomenological expression

$$I_{\text{tot}} = A^{**} A T^2 \exp \left[- \frac{q \Phi'}{k_B (T + T'_0)} \right] \times \left[\exp \left[\frac{q V_a}{k_B (T + T'_0)} \right] - 1 \right], \quad (\text{A7})$$

where the constant T'_0 is $\xi \kappa V_{b0}^{\xi-1} q / k_B$, the effective Richardson constant A^{**} is $A^* f$, and the apparent SBH, Φ' , is

$$\Phi' = \Phi_B^0 + \xi \kappa V_{b0}^{\xi-1} \ln(N_C / N_D).$$

For simplicity, the dependence of the semiconductor band gap on temperature has been ignored, and the FL position at the MS interface has been assumed to be independent of temperature.

Frequently, I - V traces at different temperatures are obtained and analyzed at a *constant current range*. Such an experimental condition may be approximated by assuming the band bending, V_{b0} , used in evaluating the ideality factor to depend on the temperature in the following fashion:

$$\beta V_{b0} = C_0, \quad (\text{A8})$$

where C_0 is a constant. It may be shown that the total current may also be approximately expressed in the phenomenological form of Eq. (A7) for a narrow range of current. However, the constant T'_0 takes the form

$$T'_0 = \frac{q \xi \kappa (2 - \xi)}{V_{bi,0}^{1-\xi} k_B},$$

and the apparent SBH, Φ' , is given by

$$\Phi' = \Phi_B^0 - \beta^{1-\xi} \kappa V_{bi,0}^{-1} C_0^{\xi} (1 - \xi) \Phi_B^0 + \beta^{1-\xi} \kappa C_0^{\xi-1} \ln \left[\frac{N_C}{N_D} \right],$$

where $V_{bi,0}^*$ is the band bending chosen for the analysis at a medium temperature.

¹E. H. Roderick and R. H. Williams, *Metal-Semiconductor Contacts* (Clarendon, Oxford, 1988).
²L. J. Brillson, *Surf. Sci. Rep.* **2**, 123 (1982).
³V. Heine, *Phys. Rev. A* **138**, 1689 (1965).
⁴J. Tersoff, *Phys. Rev. Lett.* **52**, 465 (1984).
⁵J. Bardeen, *Phys. Rev.* **71**, 717 (1947).
⁶W. E. Spicer, I. Lindau, P. Skeath, C. Y. Su, and P. W. Chye, *Phys. Rev. Lett.* **44**, 420 (1980).
⁷H. Hasegawa, L. He, H. Ohno, T. Sawada, T. Haga, Y. Abe, and H. Takahashi, *J. Vac. Sci. Technol. B* **5**, 1097 (1987).
⁸R. T. Tung, *Phys. Rev. Lett.* **52**, 461 (1984).
⁹R. J. Hauenstein, T. E. Schlesinger, T. C. McGill, B. D. Hunt, and L. J. Schowalter, *Appl. Phys. Lett.* **47**, 853 (1985).
¹⁰D. R. Heslinga, H. H. Weitering, D. P. van der Werf, T. M. Klapwijk, and T. Hibma, *Phys. Rev. Lett.* **64**, 1589 (1990).
¹¹R. T. Tung, A. F. J. Levi, J. P. Sullivan, and F. Schrey, *Phys. Rev. Lett.* **66**, 72 (1991).
¹²G. P. Das, P. Blöchl, O. K. Andersen, N. E. Christensen, and O. Gunnarsson, *Phys. Rev. Lett.* **63**, 1168 (1989).
¹³H. Fujitani and S. Asano, *Phys. Rev. B* **42**, 1696 (1990).
¹⁴J. P. A. Charlesworth, A. Oschlies, R. W. Godby, R. J. Needs, and L. J. Sham, in *Proceedings of the 20th International Conference on the Physics of Semiconductors* (World Scientific, Singapore, 1990).
¹⁵R. T. Tung, *Appl. Phys. Lett.* **58**, 2821 (1991).
¹⁶J. P. Sullivan, R. T. Tung, M. R. Pinto, and W. R. Graham, *J. Appl. Phys.* **70**, 7403 (1991).
¹⁷C. Canali, F. Catellani, S. Mantovani, and M. Prudenziati, *J. Phys. D* **10**, 2481 (1977); R. Rosenberg, M. J. Sullivan, and J.

K. Howard, in *Thin Films-Interdiffusion and Reactions*, edited by J. M. Poate, K. N. Tu, and J. W. Mayer (Wiley, New York, 1978), p. 13; I. Ohdomari, T. S. Kuan, and K. N. Tu, *J. Appl. Phys.* **50**, 7020 (1979).
¹⁸I. Ohdomari and K. N. Tu, *J. Appl. Phys.* **51**, 3735 (1980).
¹⁹J. L. Freeouf, T. N. Jackson, S. E. Laux, and J. M. Woodall, *Appl. Phys. Lett.* **40**, 634 (1982).
²⁰J. L. Freeouf, T. N. Jackson, S. E. Laux, and J. M. Woodall, *J. Vac. Sci. Technol.* **21**, 570 (1982).
²¹A. I. Bastys, V. B. Bikbaev, J. J. Vaitkus, and S. C. Karpinkas, *Litov. Fiz. Sb.* **28**, 191 (1988).
²²I. Ohdomari and H. Aochi, *Phys. Rev. B* **35**, 682 (1987).
²³R. H. Cox and H. Strack, *Solid-State Electron.* **10**, 1213 (1967).
²⁴It may be shown that an additional lowering, $\propto \gamma_1 \gamma_2^3 V_{bb}^{-1/6} D^{-3}$, is incurred to the saddle-point potential for a patch with γ_1 when it is situated at a distance D away from a second patch with γ_2 .
²⁵M. S. Tyagi, in *Metal-Semiconductor Schottky Barrier Junctions and Their Applications*, edited by B. L. Sharma (Plenum, New York, 1984).
²⁶G. Y. Robinson, in *Physics and Chemistry of III-V Compound Semiconductor Interfaces*, edited by C. M. Wilmsen (Plenum, New York, 1985).
²⁷J. H. Werner, *Appl. Phys. A* **47**, 291 (1988).
²⁸A. Y. C. Yu and E. H. Snow, *J. Appl. Phys.* **39**, 3008 (1968).
²⁹C. Barret and P. Muret, *Appl. Phys. Lett.* **42**, 890 (1983).
³⁰D. Dascalu, Gh. Brezeanu, P. A. Dan, and C. Dima, *Solid-State Electron.* **24**, 897 (1981).

- ³¹M. P. Lepselter and S. M. Sze, *Bell Syst. Tech. J.* **47**, 195 (1968).
- ³²R. T. Tung, in *Atomic Level Properties of Interface Materials*, edited by D. Wolf and S. Yip (Chapman and Hall, London, 1992).
- ³³J. P. Sullivan, R. T. Tung, F. Schrey, and W. R. Graham, *J. Vac. Sci. Technol.* (to be published).
- ³⁴F. La Via, P. Lanza, O. Viscuso, G. Fera, and E. Rimini, *Thin Solid Films* **161**, 13 (1988).
- ³⁵M. M. Atalla and R. W. Soshea, Scientific Report No. 1 (1962), Contract No. AF 19 (628)-1637, Hewlett-Packard Associated (unpublished).
- ³⁶S. M. Sze, C. R. Crowell, and D. Kahng, *J. Appl. Phys.* **35**, 2534 (1964).
- ³⁷H. C. Card and E. H. Rhoderick, *J. Phys. D* **4**, 1589 (1971).
- ³⁸R. F. Broom, *Solid-State Electron.* **14**, 1087 (1971).
- ³⁹F. A. Padovani and R. Stratton, *Solid-State Electron.* **9**, 695 (1966).
- ⁴⁰G. H. Parker, T. C. McGill, C. A. Mead, and D. Hoffman, *Solid-State Electron.* **11**, 201 (1968).
- ⁴¹J. L. Freeouf, *Appl. Phys. Lett.* **41**, 285 (1982).
- ⁴²M. Severi, E. Gabilli, S. Guerri, and G. Celloti, *J. Appl. Phys.* **48**, 1998 (1977); S. Kritzinger and K. N. Tu, *ibid.* **52**, 305 (1981); B.-Y. Tsauro, D. J. Silversmith, R. W. Mountain, L. S. Hung, S. S. Lau, and T. T. Sheng, *ibid.* **51**, 5243 (1981).
- ⁴³H. Grinolds and G. Y. Robinson, *J. Vac. Sci. Technol.* **14**, 75 (1977); N. Toyama, T. Takahashi, H. Murakami, and H. Horiyama, *Appl. Phys. Lett.* **46**, 557 (1985).
- ⁴⁴F. A. Padovani, and G. G. Sumner, *J. Appl. Phys.* **36**, 3744 (1965).
- ⁴⁵A. N. Saxena, *Surf. Sci.* **13**, 151 (1969).
- ⁴⁶B. Tuck, G. Eftekhari, and D. M. de Cogan, *J. Phys. D* **15**, 457 (1982).
- ⁴⁷J. D. Levine, *J. Appl. Phys.* **42**, 3991 (1971).
- ⁴⁸C. R. Crowell, *Solid-State Electron.* **20**, 171 (1977).
- ⁴⁹M. O. Aboelfotoh, *J. Appl. Phys.* **64**, 4046 (1988).
- ⁵⁰M. O. Aboelfotoh, *J. Appl. Phys.* **66**, 262 (1989).
- ⁵¹F. A. Padovani, in *Semiconductors and Semimetals*, edited by R. K. Willardson and A. C. Beer (Academic, New York, 1971), Vol. 7A.
- ⁵²G. S. Visweswaran and R. Sharan, *Proc. IEEE* **67**, 436 (1979).
- ⁵³B. Studer, *Solid-State Electron.* **23**, 1181 (1980).
- ⁵⁴V. B. Bikbaev, S. C. Karpinkas, and J. J. Vaitkus, *Phys. Status Solidi A* **75**, 583 (1983).
- ⁵⁵See, for example, Fig 7 of M. O. Aboelfotoh and K. N. Tu, *Phys. Rev. B* **34**, 2311 (1986).
- ⁵⁶T. Arizumi and M. Hirose, *Jpn. J. Appl. Phys.* **8**, 749 (1969).
- ⁵⁷V. W. L. Chin, J. W. V. Storey, and M. A. Green, *J. Appl. Phys.* **68**, 4127 (1990).
- ⁵⁸J. M. Andrews and M. P. Lepselter, *Solid-State Electron.* **13**, 1011 (1970).
- ⁵⁹M. Wittmer, W. Lüthy, B. Studer, and H. Melchior, *Solid-State Electron.* **24**, 141 (1981); C. J. Kircher, *ibid.* **14**, 507 (1971).
- ⁶⁰J. M. Andrews and F. B. Koch, *Solid-State Electron.* **14**, 901 (1971).
- ⁶¹A. Thanailakis and A. Rasul, *J. Phys. C* **9**, 337 (1976); E. Hökelek and G. Y. Robinson, *Solid-State Electron.* **24**, 99 (1981); N. Newman, M. van Schilfgaarde, T. Kendelwicz, M. D. Williams, and W. E. Spicer, *Phys. Rev. B* **33**, 1146 (1986); A. B. McLean and R. H. Williams, *J. Phys. C* **21**, 783 (1988).
- ⁶²R. J. Archer and T. O. Yep, *J. Appl. Phys.* **41**, 303 (1970).
- ⁶³R. T. Tung, *J. Vac. Sci. Technol. B* **2**, 465 (1984).
- ⁶⁴G. D. Mahan, *J. Appl. Phys.* **55**, 980 (1984).
- ⁶⁵H. H. Güttler and J. H. Werner, *Appl. Phys. Lett.* **56**, 1113 (1990).
- ⁶⁶J. H. Werner and H. H. Güttler, *J. Appl. Phys.* **69**, 1522 (1991).
- ⁶⁷T. Okumura and K. N. Tu, *J. Appl. Phys.* **54**, 922 (1983); O. Engstrom, H. Pettersson, and B. Sernelius, *Phys. Status Solidi A* **95**, 691 (1986); A. Tanabe, K. Konuma, N. Teranishi, S. Tohyama, and K. Masubuchi, *J. Appl. Phys.* **69**, 850 (1991).
- ⁶⁸W. J. Kaiser and L. D. Bell, *Phys. Rev. Lett.* **60**, 1406 (1988).
- ⁶⁹J. L. Freeouf, *Solid State Commun.* **33**, 1059 (1980).
- ⁷⁰L. J. Brillson, *Phys. Rev. Lett.* **40**, 260 (1978).
- ⁷¹C. J. Palmstrom, T. L. Checks, H. L. Gilchrist, J. G. Zhu, C. B. Carter, and R. E. Nahory, in *Electronic, Optical and Device Properties of Layered Structures*, edited by J. Hayes, E. R. Weber, and M. S. Hybertsen, MRS Symposia Proceedings No. EA-21 (Materials Research Society, Pittsburgh, 1990), p. 63; K. Hirose, K. Akimoto, I. Hirose, J. Mizuki, T. Mizutani, and J. Matsui, *Phys. Rev. B* **43**, 4538 (1991).